Laser treatment for corrosion prevention of electrical contact gold coating

C. Georges[a,b,*], H. Sanchez[a], N. Semmar[a], C. Boulmer-Leborgne[a],
C. Perrin[b], D. Simon[b]

[a]*GREMI, Université d'Orléans, BP6744, 45067 Orléans Cedex 2, France*
[b]*CERI-CNRS, 3A rue de la Férollerie, 45071 Orléans Cedex 2, France*

(2002)

Abstract

The materials used in electrical contact applications are constituted of a copper alloy (brass or bronze) electroplated with two coatings, a nickel layer (diffusion barrier) and a gold layer (corrosion barrier). There are some pores in the nickel and gold layers leading to corrosion of the underlying layers.

To modify the gold coating microstructure, a laser surface treatment has been undertaken. An excimer laser is used firstly because the photon absorption coefficient is larger in UV range and secondly because the laser beam homogeneity is available for a surface treatment. The purpose of this surface treatment is to suppress the porosity of the gold layer, which is responsible of the corrosion pits, and to smooth the surface as the roughness prevents a correct electrical contact.

The effects of the laser treatment are studied according to different surface parameters (roughness of the substrate, thickness of the two successive coatings, a nickel layer and a gold layer). A numerical code is used to simulate the influence of the laser beam parameter on the surface melting. Tests of corrosion are carried out in the humid synthetic air containing low contents of pollutants (NO_2, SO_2 and Cl_2). The techniques used to control these effects are optical microscopy and scanning electron microscopy (SEM).

Keywords: Laser treatment; Corrosion; Gold coating

1. Introduction

The industry of passive components takes a main part in the electronic procedures for telecommunication or computing industry. In connectors, the electrical contacts are constituted of a copper alloy (brass or bronze) covered by a nickel coating (diffusion barrier) and by a gold coating (corrosion barrier).

The study of the atmospheric corrosion mechanisms of nickel protected by gold has shown the existence of pores in the gold layer, inducing corrosion phenomena of the underlying layers [1,2]. This porosity is probably linked to the columnar crystallinestructure of the gold deposit. Nevertheless, the protection of nickel requires a perfectly tight gold coating.

To modify the structure of the gold coating, a laser surface treatment has been undertaken. The purpose of this surface treatment is to suppress the pores in the gold layer, which are responsible of the corrosion pits and to smooth the surface as the roughness prevents a correct electrical contact. The laser treatment has to

* Corresponding author. Present address: GREMI, Université d'Orléans, BP6744, 45067 Orléans Cedex 2, France.
Tel.: +33-2-38-25-7601; fax: +33-2-38-63-0271.
E-mail address: georges@cnrs-orleans.fr (C. Georges).

induce the gold layer melting without damaging the nickel underlayer. A thermokinetics model adapted to this treatment allows the study of the laser pulse duration on the melting depth of gold.

2. Experimental procedure

2.1. Laser surface treatment

The laser treatments are performed with two excimer lasers: a Lambda Physics compex 205 in KrF gas mixing configuration (λ (wavelength) = 248 nm, τ (pulse duration) = 25 ns) and a Questek XeCl (λ = 308 nm, τ = 28 ns). The choice of an excimer laser for surface treatment has been dictated by two parameters. Firstly, the UV wavelength as the photon beam penetration depth is generally lower for UV range than for larger wavelengths and this corresponds to a better photon absorption coefficient. Secondly, the beam homogeneity of the excimer laser beam allows an homogeneous surface treatment.

The laser beam is focused onto a sample, the more homogeneous part of the beam being selected by a diaphragm. The sample is fixed on a holder connected to an automatized scanner allowing an X–Y moving of the samples in front of the laser beam. The range of the laser fluence (J/cm^2) used for the surface treatment is in the range 400–600 mJ/cm^2. In order to compare the influence of the laser pulse number at the same location, 1–50 laser pulses on the same impact have been done. The size of our samples is 1 cm × 1 cm and the size of each laser impact is approximately 3 mm × 5 mm.

2.2. Types of samples

The samples are constituted of a substrate (copper alloy: brass or bronze) of 0.2 mm thickness covered with two successive coatings, a nickel layer and a gold layer. The gold coating must be deposited on a nickel underlayer in order to limit the diffusion between copper and gold. The nickel and the gold deposits are performed by electrolytic process.

The samples have different roughnesses, thicknesses in order to study the influence of these parameters on the laser treatment efficiency in relation to the corrosion tests.

- The roughness of the substrate (mirror polished or laminate polished (Ra < 0.1 μm) or laminate (Ra ≥ 0.3 μm));
- The thickness of the nickel layer (2 or 5 μm);
- The thickness of the gold layer (0.75 or 1 μm).

After laser treatment, corrosion tests were carried out with observation by optical microscopy.

2.3. Corrosion tests

The corrosion tests were carried out at 25 °C, in wet synthetic air (HR = 85%) containing three polluting gases: NO$_2$, SO$_2$ with concentrations of 0.2 vpm (volume per million, i.e. 0.2×10^{-6} litres per air litre) and of Cl$_2$ with concentration of 0.01 vpm. The test duration varies from a few days to a dozen of days. At regular intervals of time, the samples were observed to visualise the evolution of the corrosion. The photographs in Fig. 1 show the results obtained for three samples (a)–(c) of different nature. The samples in Fig. 1a and b have brass substrates with a mirror polished quality and a laminate polished quality less rough than the sample represented in Fig. 1c (laminate brass). For the sample (a), the nickel layer is 5 μm thick and the gold layer is 1 μm thick. Samples (b) and (c) have a nickel layer of 2 μm and a gold layer of 0.75 μm. On the photographs, each laser impact are represented into dotted frames. The number written in each frame corresponds to the number of laser pulses received by impact. The size of the impacts is approximately 3 mm × 5 mm but it could vary a little with the number of laser pulses.

For samples (a) and (b) it can be observed that the laser treatment has a positive effect as the aggregates (signature of the corrosion effect) in the treated zones are very much smaller and less numerous than in the untreated zones. In order to see the difference between the aggregate sizes, the enlargement of a laser treated zone and of an untreated zone for sample (b) is represented in Fig. 2.

Same scale is used for photos 2A and 2B. The laser treatment leads to a reduced size of aggregates. From corrosion test results on samples without laser treatment, it can be deduced that a sample with thicker Ni and Au layer coating has a best corrosion resistance. Conversely, this does not hold for samples irradiated by laser as deduced from results presented
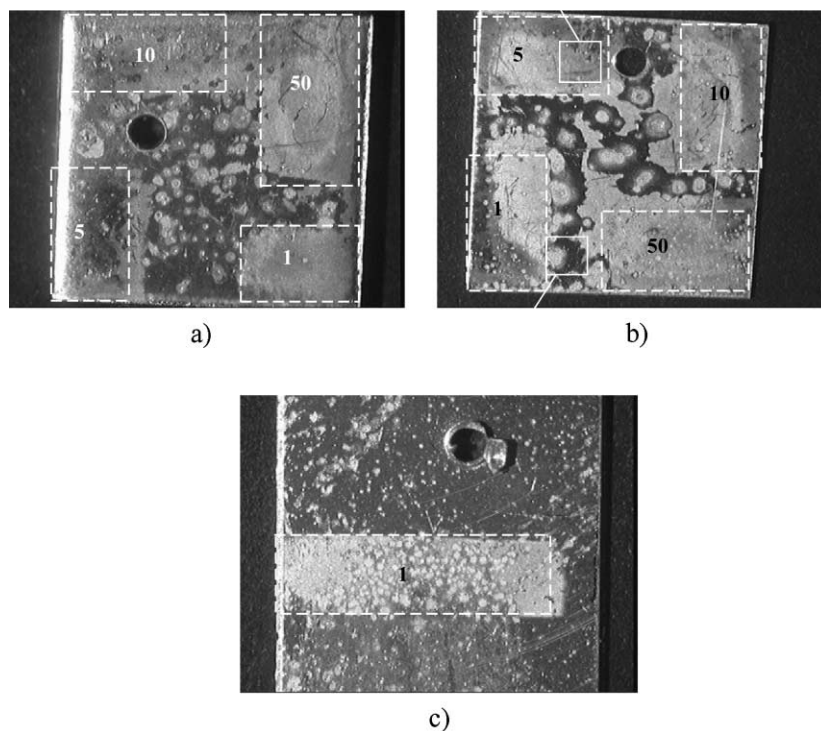
Fig. 1. Observations after laser treatment and corrosion test (331 h). Samples treated in four locations with 1, 5, 10 and 50 laser pulses by impact: (a) Ni 5 µm, Au 1 µm, Ra <0.1 µm; (b) Ni 2 µm, Au 0.75 µm, Ra <0.1 µm; (c) Ni 2 µm, Au 0.75 µm, Ra ≥0.3 µm.

in Fig. 1. Corrosion tests on irradiated parts of samples (a) and (b) lead to similar results whereas Ni and Au coating thicknesses are different. Thus, the lower coating thickness for Ni and Au layer are sufficient for corrosion resistance if a laser treatment is used as a complement to the electrolytic deposition process.

Nevertheless, for other samples with a rougher substrate like sample (c), the laser processing has no effect on the atmospheric corrosion prevention. Indeed,
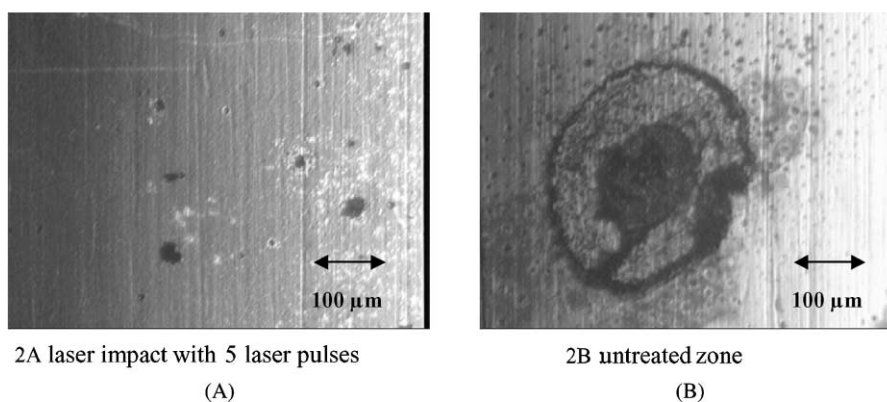

Fig. 2. Enlargements of laser treated (2A) and untreated (2B) zones.

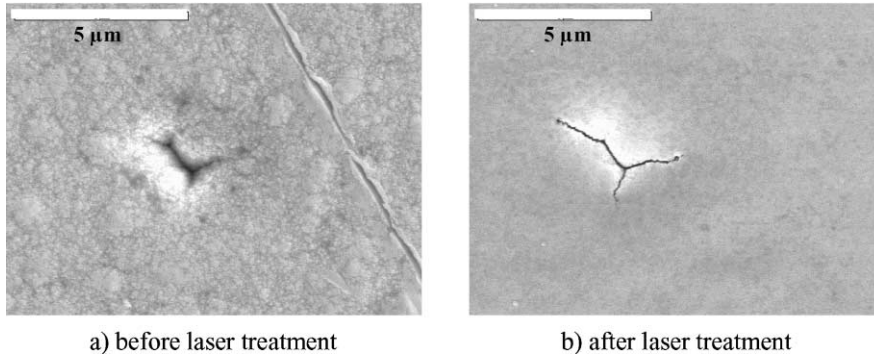a) before laser treatment   b) after laser treatment

Fig. 3. SEM observations of an identical zone before and after laser treatment.

in Fig. 1c there are many agglomerates in the laser impact. The roughness of the substrate is a limiting parameter on the quality of the laser processing: the roughness cannot exceed 0.1 μm.

2.4. Tests of porosity

In order to estimate the efficiency of the laser treatment for porosity vanishing, some holes have been chemically produced on the gold layer. Indeed SEM cannot evidence pores as their sizes are in the nanometer range. Fig. 3a presents a SEM view of a sample surface with a hole reaching the nickel layer and a scratch on the gold layer. To obtain the hole, the sample has been submitted to nitrous atmosphere for 10–30 min and products have been dissolved in water then in ammoniac. The SEM observation of this zone after laser processing shows the evolution of surface defects according to their sizes (Fig. 3b). Results are obtained with the laser XeCl ($\tau = 28$ ns) on mirror polished samples.

It can be noted that the laser treatment smoothes the surface and eliminates the scratch into the thickness of the gold layer. For more significant and major defects as our voluntary holes reaching the nickel layer, there is no remaining but conversely an enlarging of the damage. The defects larger than 1 μm in depth cannot be eliminated.

2.5. Laser parameters

The parameters of the lasers (fluence, pulse number, pulse duration) influence the efficiency of the processing. Indeed, the experimental results allow to conclude that the whole gold layer must be melted in a uniform way in depth and on surface in order to suppress all the pores. For the number of laser pulses, the best results are obtained for a number of pulses ranging from 1 to 5. The laser fluence, which is the laser energy deposited per unit of area (J/cm^2) must be sufficient to melt the gold layer without vaporisation, and must be in the range 400–600 mJ/cm^2.

The melting of the gold layer is a thermal process: the laser pulse duration τ influences the lifetime and the depth of the molten bath. τ is a fixed parameter for a given laser. We have noticed that the excimer laser XeCl with $\tau = 28$ ns gives better results in corrosion resistance than the excimer laser KrF with $\tau = 25$ ns. It would be necessary to have more pulse time difference to study the influence of this parameter, and calculations of the molten depth of the gold layer with a 1D thermokinetic model have been performed.

3. Modelling

Despite the ultra-fast pulsed interaction between laser beam and surface coating (25 ns), heat diffusion inside the coating material is described by the one dimension heat equation (1). Relaxation times of electron–electron and electron–phonon collisions are close to 10^{-12} and 10^{-14} s, respectively. Thus, no additional time derivation term is added [3].

$$\frac{1}{\alpha}\frac{\partial T}{\partial t} = \frac{\partial^2 T}{\partial x^2} \qquad (1)$$

where α is the thermal diffusivity. Shortly after the interaction, the surface temperature rises dramatically to large values inducing surface melting. Two zones are then considered. The first zone (zone I) is the solid phase heat conduction. The thermal problem is then treated as a semi-infinite slab and the surface temperature remains below the melting one. An exact analytical solution is easily written. When the surface temperature rises over the melting point (T_M), the liquid/solid zone (phase change) occurs. In this second zone (II), the thermal problem is resolved by a linearisation of the temperature expression as proposed in [4]. Then it is possible to compute the heat flux density to obtain the melting front location ($\xi(t)$).

Boundary conditions related to the two distinct zones are summarised as following:

$$T_S(0, x) = T_0, \quad t = 0, \quad -k_S \frac{\partial T_S}{\partial x} = \varphi(t),$$
$$x = 0, \quad T_S(t, \infty) = T_0, \quad x \to \infty \quad (2)$$

$$T_S(0, x) = T_0, \quad t = 0, \quad -k_L \frac{\partial T_L}{\partial x} = \varphi(t),$$
$$x = 0, \quad T_S(t, \xi) = T_L(t, \xi) = T_M,$$
$$x = \xi(t), \quad T_S(t, \infty) = T_0, \quad x \to \infty \quad (3)$$

The boundary conditions for $t = 0$ and $x \to \infty$ are expressed by room temperature (T_0). The condition at the immediate surface ($x = 0$) is expressed by the absorption of heat flux density. Experimental evaluation of $a(T)$ (absorption coefficient) and $\varphi(t)$ is discussed in thermal properties and experiment part. All these boundary conditions are valid in both zones (I and II).

Moreover, the temperature equilibrium is written at the melting position ($x = \xi(t)$) to ensure the continuity of thermal field. However, at the same position, the heat flux balance expressed by relation (4) must take into account the latent heat flux.

$$\varphi_L - \varphi_S|_{x=\xi(t)} = \left(-k_L \frac{\partial T_L}{\partial x}\right) - \left(-k_S \frac{\partial T_S}{\partial x}\right)\Bigg|_{x=\xi t}$$
$$= \rho_L L_M \frac{d\xi}{dt} \quad (4)$$

To achieve the thermal modelling, we underline the permutation of the boundary conditions for the solid state heat diffusion when considering either zone I or II. When considering the liquid and solid phases an equal mass density, and neglecting the sensitive heat flux in the liquid phase, we are able to evaluate easily the melting speed $d\xi/dt$ by using an approximation of relation (4). In the liquid phase, the Kantorovich method [4] resolves the mathematical system composed by relationships (1)–(4).

In this first step of calculation, the values of thermal conductivity (k) and diffusivity (α) of gold are extracted from Touloukian data base [5] (see Table 1). They are averaged on the two characteristic temperature ranges: from $T_0 = 300\,\text{K}$ to T_M (melting temperature) $= 1337\,\text{K}$ for the solid state and from $T_M = 1337\,\text{K}$ to T_E (boiling temperature) $= 3353\,\text{K}$ for the liquid state. The specific heat (C_P) and mass density (ρ) are the averaged solid state ones. The melting latent heat is considered at normal pressure and equals to $64\,270\,\text{J kg}^{-1}$.

A calorimetric method is employed to determine the absorption coefficient on the surface coating. Thus, it can be proposed $a = 0.7$.

The temporal shape of the laser pulse power density has been recorded by a photodiode. The function $\varphi(t)$ given by Eq. (5) is used to fit this experimental intensity distribution (see Fig. 4).

$$\frac{\overline{\varphi(t)}}{\varphi_0} = \frac{1}{[1 + \omega^2(1/t^* - t^*)^2]}, \quad t^* = \frac{t}{\tau} \quad (5)$$

Table 1
Thermophysical properties of gold

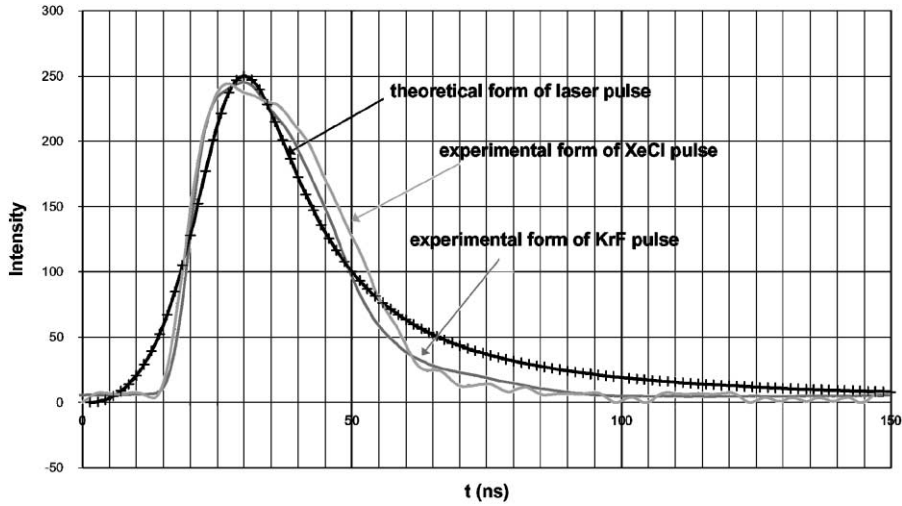|	T (temperature) (K)	k (thermal conductivity) (W m^{-1} K^{-1})	α (thermal diffusivity) (m^2 s^{-1})	C_P (specific heat) (J kg^{-1} K^{-1})	ρ (mass density) (kg m^{-3})	a (absorption coefficient) (W W^{-1})
Au (solid state)	300–1337	280	1.0×10^{-4}	170	16 500	0.7
Au (liquid state)	1337–3353	150	0.5×10^{-4}	–	16 500	0.7

Fig. 4. Temporal distribution of both laser pulses and the function $\varphi(t)$.

Parameters ω and φ_0 allows accommodating the theoretical curve to experimental pulse shapes of both excimer lasers. The theoretical curve is represented in Fig. 4.

The thermal modelling can consequently be used to determine the laser fluence range allowing the gold coating melting without vaporisation. The melting thickness can be deduced for different laser fluences.

As shown in Fig. 5, the lower laser fluence ($F = 390 \, \text{mJ/cm}^2$) is the threshold value for gold coating melting and the total melting of the gold layer
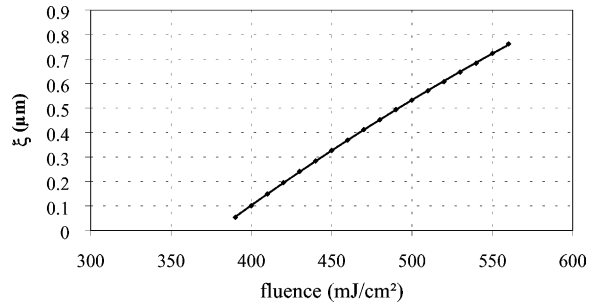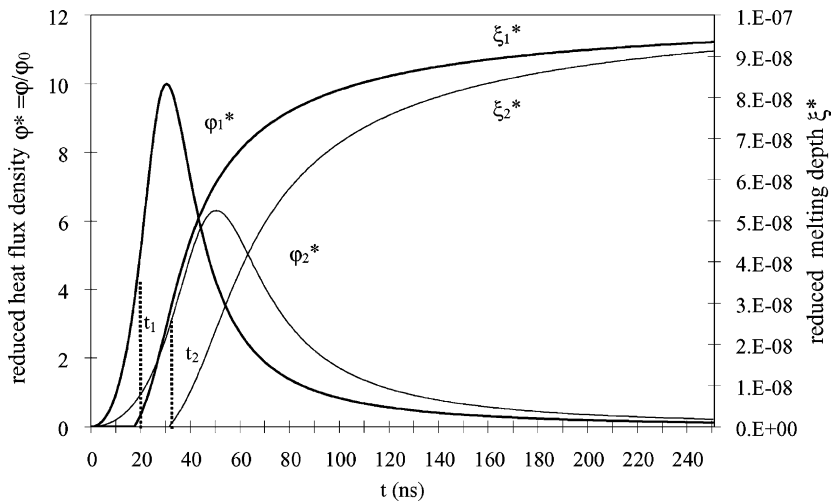

Fig. 5. Melting depth versus laser fluence.

Fig. 6. Melting depth versus time for a fixed fluence.

(0.75 μm thick) is obtained for a fluence of 560 mJ/cm^2. These values are in agreement with the experimental results as detailed in Section 2.5.

Fig. 6 gives the result of the simulation for two different pulse shapes corresponding to the same laser fluence (500 mJ/cm^2) but to two distinguished pulse time durations ($\tau_1 = 30$ ns and $\tau_2 = 50$ ns). For the same fluence, when considering two different heat density shapes [$\varphi_1^*(t)$, $\varphi_2^*(t)$], the melting depth [$\xi_1^*(\lambda)$, $\xi_2^*(\lambda)$] evolves distinguishably. By varying the parameters φ_0 and ω of the function $\varphi(t)$ (Eq. (5)) it can be evidenced that the melting depth strongly depends on the laser pulse shape. In this computation, the heat diffusion is included only in the conduction phase until the melting temperature (corresponding times: $t_1 = 18$ ns and $t_2 = 32$ ns). In the second thermal process (melting) a global heat balance is considered to evaluate the melting depth. Notice that for fluence values below the critic ones (ebullition threshold), the melting is more important when the pulse duration is shorter. However, when the values are above the ebullition threshold, the melting depth curves evolves inversely. This case study will be developed in a next work. These simulation results suppose that is possible to increase the melting time even if working over the critic values by increasing the pulse duration.

4. Conclusion

Laser melting can remove the porosity of a gold layer prepared by electrolytic process. This treatment is more efficient on samples with mirror polished or laminate polished substrates. As shown in the simulation part, by increasing the laser pulse time the complete melting of the gold layer can be achieved and all the porosity can be eliminated. Nevertheless, the roughness of the substrate induces defects in the nickel and gold coating that cannot be recovered by a laser melting process.

References

[1] C. Perrin, D. Simon, J. Chim. Phys. 96 (1999) 1226–1244.
[2] I. Odvenall, C. Leygraf, J. Elecrochem. Soc. 144 (10) (1997) 3518–3525.
[3] P. Guillemet, J.-P. Bardon, C. Rauch, Int. J. Heat Mass Transf. 40 (17) (1997) 4043–4053.
[4] N. Ozisik, Heat Conduction, Wiley, New York, 1993.
[5] Y.S. Touloukian, T. Makita, Thermal Properties of Matter, Plenum, New York, 1970.